

Electronic structure of alkali-metal fluorides, oxides, and nitrides: Density-functional calculations including self-interaction corrections

Björn Baumeier,* Peter Krüger, and Johannes Pollmann

Institut für Festkörpertheorie, Westfälische Wilhelms-Universität Münster, D-48149 Münster, Germany

Grigori V. Vajenine

Max-Planck-Institut für Festkörperforschung, D-70569 Stuttgart, Germany

and Institut für Anorganische Chemie, Universität Stuttgart, D-70569 Stuttgart, Germany

(Received 25 June 2008; revised manuscript received 3 September 2008; published 23 September 2008)

The recently synthesized compound Na_3N has experimentally been shown to be semiconducting much in contrast to the outcome of standard density-functional theory calculations which find Na_3N to be metallic. To address this obvious contradiction, we have systematically investigated the electronic structure of Na_3N by density-functional calculations employing self-interaction-corrected pseudopotentials which have been shown before to yield results in much better agreement with experiment than standard local-density calculations. To assess the usefulness of such pseudopotentials for a broader class of related materials, we have carried out, in addition, a comparative *ab initio* study of the electronic structure of the nine alkali-metal fluorides MF, oxides M_2O , and nitrides M_3N with $\text{M}=\text{Li}$, Na , and K . We arrive at valence and conduction bands that are in good agreement with the restricted results available in the literature from calculations going beyond the local-density approximation and from experiment. In particular, Na_3N turns out to be clearly semiconducting, as observed in experiment.

DOI: [10.1103/PhysRevB.78.125111](https://doi.org/10.1103/PhysRevB.78.125111)

PACS number(s): 71.20.Ps, 71.15.Mb

I. INTRODUCTION

Several years ago, Fischer and Jansen¹ reported the anti- ReO_3 structure for films of metastable sodium nitride (Na_3N) deposited at low temperatures. Recently single crystalline and polycrystalline Na_3N have been synthesized successfully on a laboratory scale by reaction of metallic sodium or a liquid Na-K alloy with plasma-activated nitrogen,² thus allowing for an intensive experimental investigation of its structural and optical properties employing powder and single-crystal x-ray diffraction and optical absorption.³ Based on the respective preliminary experimental data, Na_3N appears to be semiconducting with a band gap of 1.6 eV. On the contrary, concomitant band-structure calculations² based on density-functional theory (DFT) within local-density approximation (LDA) have yielded a *negative* gap of 0.6 eV. This theoretically predicted metallicity of Na_3N is in obvious contrast to the experimental data and the expected formulation as $(\text{Na}^+)_3\text{N}^{3-}$.

Now it is well known that the description of electronic properties of insulators and semiconductors within the framework of DFT-LDA suffers from the systematic underestimation of the fundamental band gap. These deviations can partially be traced back to unphysical self-interactions inherent in LDA, as shown by Perdew and Zunger.⁴ For atomic systems the latter authors proposed a self-interaction-correction (SIC) scheme and succeeded in overcoming the problems of the LDA to a large extent. These corrections are state dependent, however, so that a direct application of this approach to bulk solids is computationally very demanding. Nevertheless, full SIC calculations, in which more or less localized orbitals are calculated in a self-consistent way, have been carried out with great success, e.g., for transition metals by Svane *et al.*,⁵ for high- T_c superconductors by Temmerman and co-workers^{6,7} and for transition-metal oxides by

Arai and Fujiwara.⁸ Thereafter, several approaches have been developed to transfer the effects of the atomic SIC to the solid approximately.⁹⁻¹³ Here we follow the scheme based on Refs. 9 and 12 in constructing self-interaction-corrected pseudopotentials for the solids at hand. Using SIC pseudopotentials in DFT calculations has resulted in significant improvements in the description of both bulk and surface electronic properties, as compared to standard DFT-LDA results for IIB-VI compound semiconductors,⁹ group-III nitrides,¹⁰ silicon carbide,¹² and alkaline-earth metal oxides.¹⁴ Also the description of the properties of isolated monolayers as well as nanotubes of SiC, BN, and BeO has greatly been improved.¹⁵ Based on these achievements, we expect the SIC approach to be also useful in reconciling the apparent contradiction between the computed metallic LDA band structure and the observed semiconducting properties of Na_3N .

To scrutinize the use of SIC pseudopotentials for the broader class of lithium, sodium, and potassium fluorides, oxides and nitrides, we also perform a comparative study of the \mathbf{k} -dependent electronic structure of these related compounds ranging from wide-band-gap insulators possibly to metals. For the fluorides, in particular, and less so for the oxides, there are data in the literature to which we can compare our DFT-SIC results. As it turns out, DFT-SIC yields electronic band structures for the alkali-metal fluorides and oxides that are in good agreement with experimental data and theoretical results of *GW* quasiparticle calculations. Based on this agreement, we expect that the DFT-SIC approach also yields significant improvements over DFT-LDA calculations concerning the electronic structure of Li_3N , Na_3N , and K_3N .

The paper is organized as follows. In Sec. II, we summarize the methodology of our calculations. In Sec. III, we first briefly address DFT-SIC calculations for the involved atoms before we turn to a detailed discussion of the electronic

structure of the studied alkali-metal fluorides, oxides, and nitrides. Calculated structural properties of these materials are briefly addressed in the Appendix. A short summary concludes the paper.

II. METHODOLOGY

Standard LDA calculations constitute the reference point for our investigations. In these calculations we employ non-local, norm-conserving *ab initio* pseudopotentials in separable Kleinman-Bylander form¹⁶ and use the exchange-correlation functional of Ceperley and Alder,¹⁷ as parameterized by Perdew and Zunger.⁴ The standard pseudopotentials are constructed according to the prescription of Hamann.¹⁸ For the alkali-metal atoms, partial nonlinear core corrections, as introduced by Louie *et al.*,¹⁹ are included. The wave functions are expanded employing a basis set of atom-centered Gaussian orbitals with several shells of *s*, *p*, *d*, and *s** symmetry per atom with appropriately determined decay constants.²⁰ Since we deal with some relatively low-density substances for the oxides and especially the nitrides, we place additional slowly-decaying *s*-like Gaussian orbitals in the empty regions in order to allow for a satisfying description of extended bulk states. To overcome the usual LDA shortcomings in describing electronic properties we employ our SIC approach.^{9,10,12,14} First, we perform atomic SIC calculations based on the prescription of Perdew and Zunger.⁴ The resulting angular-momentum dependent self-interaction-corrected pseudopotentials are then transferred to the solid¹² and are represented in separable Kleinman-Bylander form. Brillouin-zone integrations are performed using special *k*-point sets in the irreducible wedge generated according to the prescription of Monkhorst and Pack.²¹ The number of *k* points was tested to yield convergent results.²²

III. RESULTS

In this section, we first shortly summarize our results for the isolated atoms. These constitute the starting point for the construction of the self-interaction-corrected pseudopotentials. Thereafter, we address the electronic structure of bulk Li, Na, and K fluorides, oxides, and nitrides, respectively, in detail.

A. Atomic term values

In Table I we compare the term values of the different atomic levels, resulting from our SIC and LDA calculations with one another and with experimental ionization energies.

The results show that the *s* levels of the valence shell of the alkali metals experience significantly lower self-interaction corrections $\Delta\epsilon$ than the *2s* and *2p* levels of N, O, and F, respectively. This difference gives rise to a significant shift of the related bands in the fluorides, oxides, and nitrides and consequently, the gap can be expected to open up in these materials due to self-interaction corrections, as compared to the LDA results. It should be noted that the term values of the highest occupied *s* levels of Li, Na, and K, resulting from the SIC calculations, agree with the experimental ionization energies within better than 0.3 eV. In con-

TABLE I. Atomic term values (in eV) for Li, Na, K, N, O, and F atoms resulting from our non-spin-polarized SIC and LDA calculations. Additionally, the energy shifts $\Delta\epsilon = \epsilon^{\text{SIC}} - \epsilon^{\text{LDA}}$ of the term values due to self-interaction correction are given. Experimental ionization energies for the highest occupied levels from Ref. 23 are listed for comparison.

Element	Level	$E_{\text{ion}}^{\text{exp}}$	ϵ^{SIC}	ϵ^{LDA}	$\Delta\epsilon$
Li	<i>2s</i>	-5.39	-5.10	-2.90	-2.20
Na	<i>3s</i>	-5.14	-4.92	-2.82	-2.10
K	<i>4s</i>	-4.34	-4.06	-2.42	-1.64
N	<i>2s</i>		-25.06	-18.41	-6.65
	<i>2p</i>	-14.53	-13.47	-7.24	-6.23
O	<i>2s</i>		-31.38	-23.74	-7.64
	<i>2p</i>	-13.62	-16.48	-9.20	-7.28
F	<i>2s</i>		-38.28	-29.63	-8.65
	<i>2p</i>	-17.42	-19.60	-11.29	-8.31

trast, the LDA term values deviate from the experimental data by 2.49, 2.32, and 1.92 eV, respectively. The *2p* levels of N, O, and F resulting from our SIC calculations appear to deviate stronger from experiment than the alkali-metal term values calculated within SIC. A direct comparison of the measured *2p* ionization energies with our values in Table I is misleading, however, since the latter are obtained from non-spin-polarized calculations while the former include spin polarization. For the bulk crystals investigated in this work, spin polarization is irrelevant since the respective levels are non-spin polarized in the solids. Taking spin polarization into account we obtain atomic term values of -14.73 eV for N_{2*p*}, -13.77 eV for O_{2*p*}, and -18.09 eV for F_{2*p*}. These values agree with experiment (see Table I) within 0.20, 0.15, and 0.67 eV, respectively, lending further support to the appropriateness of our results for the non-spin-polarized term values which apply in the solids. It is only fair to note at this point that ionization energies can be calculated directly within LDA by evaluating the difference between the ground-state energies of the neutral and the singly-ionized atoms (so-called ΔSCF calculations) yielding good agreement with experiment.²⁴

Starting out from this significantly improved description of the underlying atomic term values we construct self-interaction-corrected pseudopotentials²⁵ according to Ref. 12 and study the bulk electronic structure of the above mentioned alkali-metal fluorides, oxides, and nitrides. To allow for a clear identification of the SIC effects on the LDA band structures, we evaluate both at the same, namely the experimental lattice constants which we consider to be the most realistic. Theoretical LDA and SIC lattice constants and their effect on the band gaps are briefly addressed in the Appendix.

B. Bulk electronic structure

The results of the SIC calculations for the nine bulk crystals are summarized in Figs. 1–3 and Table II, which we repeatedly refer to in the course of the following discussion.

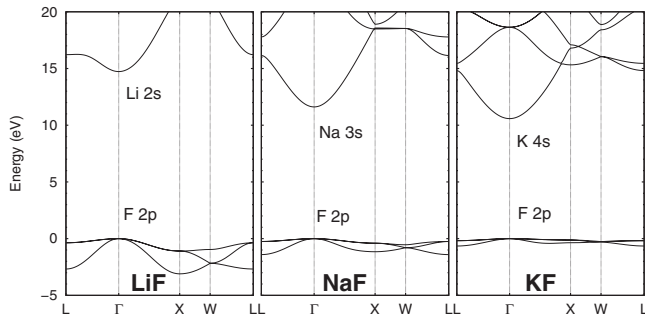


FIG. 1. Electronic band structures of LiF, NaF, KF resulting from SIC calculations.

1. Fluorides

All three fluorides crystallize in the sodium-chloride structure (space group $Fm\bar{3}m$) with lattice constants of 3.99 Å (LiF), 4.57 Å (NaF), and 5.29 Å (KF), respectively.³⁶ The calculated SIC band structures for the three fluorides are shown in Fig. 1. In these highly ionic compounds the valence bands are basically anion-derived consisting of one low-lying F 2s band (not shown in Fig. 1) and three F 2p bands defining the top of the valence bands (see Fig. 1). These groups of bands are separated in energy by a large ionic gap. The lowest conduction bands are mostly cationic s bands. All three compounds are ionic insulators having direct band gaps at Γ of 14.7 eV (LiF), 11.6 eV (NaF), and 10.6 eV (KF), respectively, according to our DFT-SIC results. The band gaps and average F 2s band positions, resulting from our DFT-LDA and DFT-SIC calculations are summarized in Table II. Experimental gap energies from optical reflection and absorption measurements^{3,26–35} are given in the table for comparison. Those for the fluorides are significantly underestimated by some 6 eV within DFT-LDA, while our DFT-SIC results are in very good accord with experiment constituting a significant improvement over DFT-LDA. In addition, our DFT-SIC band gaps are in reasonable agreement with other theoretical results from correlation-corrected Hartree-Fock calculations^{37–39} ranging from 14.0 to 16.5 eV for LiF, 12.0 to 14.7 eV for NaF, and 10.9 to 13.3 eV for KF. To the best of our knowledge, results of quasiparticle calculations have only been reported for LiF,^{27,40,41} to date. The authors find a quasiparticle gap of 14.4, 14.3, and 14.3 eV, respectively, which is close to our

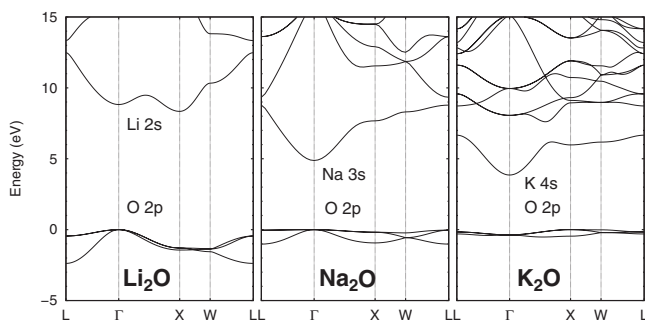


FIG. 2. Electronic band structures of Li₂O, Na₂O, K₂O resulting from SIC calculations.

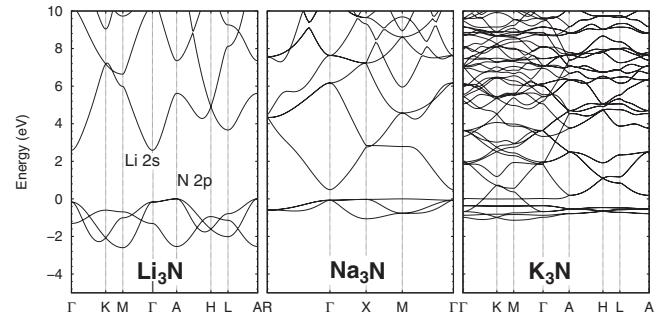


FIG. 3. Electronic band structures of Li₃N, Na₃N, K₃N resulting from SIC calculations.

calculated gap of 14.7 eV. In this context it appears worth mentioning that our DFT-SIC calculations are numerically not more involved than any standard DFT-LDA calculation.

An earlier SIC study⁴² arrived at band gaps of 16.6, 13.3, and 12.5 eV for LiF, NaF, and KF, respectively, overestimating the experimental values. In this study, an *ad hoc* ansatz is made for corrective SIC potential terms and the single-particle charge densities are evaluated using approximate Wannier functions. The variational freedom of the single-particle orbitals is limited in this approach, however, which could be one reason for the slightly overestimated band gaps.

Along with the reduction in the gap energy from LiF to KF, we also find a narrowing of the width of the F 2p valence bands from 3.1 eV in LiF over 1.4 eV in NaF to 0.6 eV in KF (see Fig. 1). They are mainly formed by F_{2p} states. There is only a negligible admixture from cation s states. Therefore, the dispersion of the F 2p bands originates almost

TABLE II. Calculated gap energies and average energetic position of the anion s band (in eV) resulting from our LDA and SIC calculations in comparison with experimental results.

	Band gap			Anion s-band	
	LDA	SIC	Expt.	LDA	SIC
LiF	8.5	14.7	13.6, ^a 14.2, ^b 14.5 ^c	-21.3	-21.5
NaF	5.7	11.6	11.5, ^a 11.7 ^d	-20.2	-20.5
KF	5.2	10.6	10.8, ^e 10.9, ^f 11.0 ^g	-20.1	-20.4
Li ₂ O	4.8	8.3	8.0 ^h	-15.2	-16.0
Na ₂ O	1.8	4.9	(4.4–5.8) ⁱ	-14.3	-14.6
K ₂ O	1.1	3.8	(4.0–5.4) ⁱ	-14.1	-15.0
Li ₃ N	1.1	2.6	2.2 ^j	-11.2	-11.8
Na ₃ N	0.0	0.5	1.6 ^k	-10.8	-10.8
K ₃ N	0.0	0.0		-11.6	-11.3

^afrom Ref. 26.

^bfrom Ref. 27.

^cfrom Ref. 28.

^dfrom Ref. 29.

^efrom Ref. 30.

^ffrom Ref. 31.

^gfrom Ref. 32.

^hfrom Ref. 33.

ⁱ(lower–upper) limits (from Ref. 34–estimated), see text.

^jfrom Ref. 35.

^kfrom Ref. 3.

exclusively from direct interactions between the anions which are second-nearest neighbors in the lattice. The increasing size of the cations increases the anion-anion distance from 2.85 Å for LiF over 3.25 Å for NaF to 3.85 Å for KF so that the anion-anion interaction and the F $2p$ -bandwidths decrease accordingly. The same trend was also observed in ultraviolet photoemission spectroscopy experiments.⁴³ Concerning absolute values, we note that Shirley *et al.*²⁷ found for LiF a corresponding bandwidth of 3.5 and 3.6 eV from experiment and theory, respectively. For NaF, Wertheim *et al.*⁴⁴ observed a width of 1.6 ± 0.2 eV. Our results are in satisfactory agreement with these data.

2. Oxides

Li_2O , Na_2O , and K_2O all crystallize in the cubic antiperovskite structure (space group $Fm\bar{3}m$), which is antiperovskite to CaF_2 . Positive alkali-metal ions are arranged on a simple-cubic lattice with a spacing of $a/2$. Alternating cube centers are occupied by O^{2-} ions. The lattice constants are 4.62, 5.56, and 6.45 Å, respectively.⁴⁵ As these lattices are comparatively open structures, we include additional slowly-decaying s orbitals at $\frac{a}{2}(1, 1, 1)$ in order to appropriately represent extended cation-derived states in the solid. The resulting fundamental band gaps and oxide s -band positions are listed in Table II, as well. Experimental data on the value of the band gap are relatively sparse. For Li_2O there is a more recent reflectivity study³³ in which the authors derived a fundamental band gap of 8.0 eV from excitonic spectra. The only reported equivalent for Na_2O and K_2O is a very early study of corresponding absorption spectra³⁴ showing transitions at 6.6, 4.4, and 4.0 eV for Li_2O , Na_2O and K_2O , respectively. These spectra, however, contain excitonic contributions which have not been accounted for in Ref. 34. Considering that the result for Li_2O of 6.6 eV deviates from the more recent exciton-corrected value in Ref. 33 by 1.4 eV, a very rough estimate for the upper limit of the expected Na_2O and K_2O gaps can be made by adding this full difference to the reported values for Na_2O and K_2O in Ref. 34. The resulting values of 5.8 eV (Na_2O) and 5.4 eV (K_2O) are given in Table II as upper limits, as well. Certainly, the true gaps in the two latter cases are smaller than the upper limits given in Table II since the exciton energies in Na_2O and K_2O are bound to be considerably smaller than in Li_2O because the oxides of sodium and potassium have significantly smaller energy gaps than Li_2O (see Fig. 2). So for Na_2O one would expect the gap to be considerably closer to the lower limit and for K_2O it ought to be very close to the lower limit. It is obvious (see Table II) that for all three alkali-metal oxides, the band gaps calculated within DFT-LDA show the usual strong underestimation of the measured gap energies while the SIC gaps are opened up considerably being in much better agreement with experiment.

Figure 2 shows the calculated SIC band structures for the three oxides. In all three cases, a low-lying O $2s$ band (not shown in the figures) occurs (see Table II). Near the top of the valence bands we find a group of three O $2p$ bands whose widths decrease again from Li_2O to K_2O . The bottom of the conduction bands originates in each case from cation ns states with $n=2, 3$, and 4, respectively. For Li_2O , we find

a band gap of 8.3 eV in nice agreement with the experimental value³³ of 8.0 eV and the gap energy of 8.1 eV resulting from a hybrid-functional calculation.⁴⁶ The band gap is indirect, with the valence-band maximum located at Γ and the conduction-band minimum at X . In contrast, Na_2O has a direct gap at Γ , which is 4.9 eV wide according to our SIC results. The situation is different again for K_2O . Here the results show an indirect fundamental gap of 3.8 eV between X and Γ . Similar observations regarding the nature of the band gaps have recently been reported by Eithiraj *et al.*⁴⁷ based on a TB-LMTO study. Their calculated LDA band gaps of 5.8 eV for Li_2O , 2.4 eV for Na_2O , and 1.8 eV for K_2O are considerably lower, however.

The valence electronic structure of the alkali-metal oxides has been studied experimentally by Mikajlo and co-workers using electron momentum spectroscopy.⁴⁸⁻⁵⁰ In particular, the authors derived the width of the upper O $2p$ valence bands to be 1.6 eV for Li_2O , 0.6 eV for Na_2O , and 0.3 eV for K_2O with an uncertainty of ± 0.2 eV each. The respective values from our SIC calculations of 2.4, 1.0, and 0.5 eV are in reasonable accord with the data.

3. Nitrides

Lithium nitride (Li_3N) crystallizes in a hexagonal structure with the space group $P6/mmm$. In this peculiar structure each N atom is surrounded by eight Li atoms in a layered configuration along the hexagonal axis consisting of one Li_2N layer and a layer of pure Li. The lattice constants⁵¹ are $a=3.65$ Å and $c=3.87$ Å. Accounting for the unique character of the atomic structure of Li_3N , we place additional slowly-decaying Gaussian orbitals at $(a/2, \pm a/2\sqrt{3}, c/2)$, i.e., at positions within the Li layer above and below Li atoms of the Li_2N layer, to accurately represent the more extended bulk states. From optical-absorption experiments^{35,52} a gap energy of about 2.2 eV was obtained. In contrast, our calculated LDA gap energy is only 1.1 eV (see Table II) in agreement with the results of previous DFT-LDA studies.^{53,54} In earlier Hartree-Fock calculations,⁵⁵ a gap energy of 7.8 eV was obtained.

In the left panel of Fig. 3 the band structure of Li_3N resulting from our SIC calculations is shown along the high-symmetry lines of the hexagonal Brillouin zone. Also Li_3N has a low-lying anionic N $2s$ valence band (see Table II) and three N $2p$ bands near the top of the valence bands. The lowest conduction band is mainly derived from Li_{2s} states. The band structure shows an indirect band gap between the A and Γ points. The gap is 2.6 eV wide and deviates only by 0.4 eV from the experimental value³⁵ of 2.2 eV. As a consequence of the hexagonal structure, a crystal-field splitting occurs for the highest N $2p$ bands at the Γ point. While the components perpendicular to the hexagonal axis remain degenerate, the p_z component is shifted down in energy showing an inverted dispersion. The crystal-field splitting is rather large amounting to 1.2 eV.

Contrary to Li_3N , sodium nitride (Na_3N) was experimentally found to occur in a cubic anti- ReO_3 crystal structure (space group $Pm\bar{3}m$) with a lattice constant² of 4.73 Å. This structure (see Fig. 4) can be interpreted as a cubic perovskite (CaTiO_3) structure with a removed Ca atom so that the N

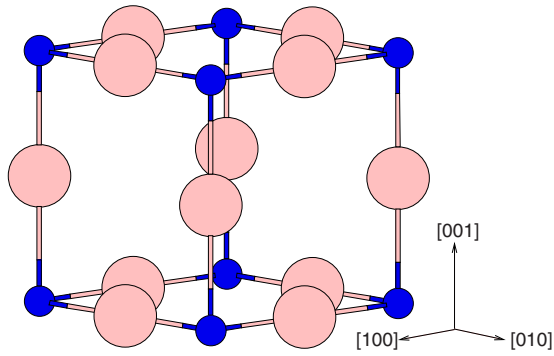


FIG. 4. (Color online) Lattice structure of Na_3N . Positions of the Na (N) atoms are indicated by large (small blue) circles.

atoms are located in the Ti sites while the Na atoms occupy the O sites. Slowly decaying Gaussian orbitals are placed on the cube centers. As noted before, standard LDA calculations yield an electronic structure with a negative gap of 0.6 eV for this crystal rendering Na_3N metallic. The band structure of Na_3N resulting from our SIC calculations is shown in the middle panel of Fig. 3.

Compared to the band structure of Li_3N , the energy separation between the top of the N $2p$ valence bands and the bottom of the Na $3s$ conduction band has decreased considerably. Yet, Na_3N clearly exhibits a band gap of 0.5 eV in our SIC results while it appears to be a metal within DFT-LDA. Nevertheless, it should be noted that the calculated SIC gap is significantly smaller than the measured gap (1.6 eV). The width of the three N $2p$ bands has strongly decreased, as compared to Li_3N . The reason appears to be more subtle than, e.g., for the respective fluorides. The anion-anion distance is as large as 4.73 Å, indeed, but the anion-cation interaction in the N-Na-N bridges (see Fig. 4) comes into play in Na_3N . This can happen, since the Na_{3s} bands at Γ are relatively close in energy to the N_{2p} bands allowing for a certain interaction.

In order to elucidate the origin of the metallicity resulting within LDA we show the LDA band structure of Na_3N in the left panel of Fig. 5. In the figure we have marked bands according to their orbital character, resulting from a Mullikan

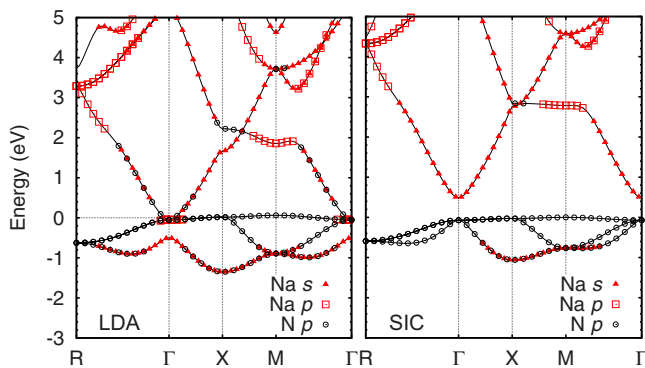


FIG. 5. (Color online) Band structure of Na_3N resulting from LDA (left panel) and SIC calculations (right panel), respectively. Bands derived from N_{2p} states are marked by open circles. Red triangles and squares label bands that are derived from Na_{3s} and Na_{3p} states, respectively.

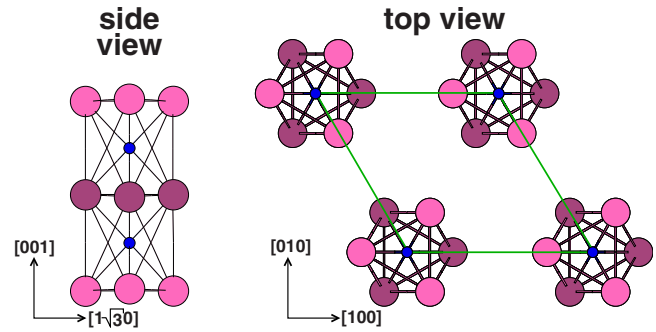


FIG. 6. (Color online) Side view of a single K_3N column and top view of the arrangement of the columns in the hexagonal anti- TiI_3 crystal structure. Positions of the K and N atoms are indicated by light and dark red (light and dark gray) and blue (black) circles, respectively. The green (gray) line represents the boundary of the basal plane of the unit cell.

analysis. Bands that can uniquely be identified as being derived from N_{2p} states are marked by open circles. Red filled triangles and open squares label bands that are derived from Na_{3s} and Na_{3p} states, respectively. It becomes clear that the metallic character of Na_3N resulting within LDA originates from an overlap of the Na $3s$ with the occupied N $2p$ bands occurring at the Γ point of the cubic Brillouin zone. This leads to a significant mixture of the two orbital contributions throughout the Brillouin zone. One of the three former N $2p$ bands is pushed down in energy due to nonvanishing contributions from Na_{3s} states. At the same time, the anionic $2p$ states also mix with the cationic $3s$ states for energies above the Fermi level, as can clearly be seen in the left panel of Fig. 5. This figure also indicates that Na_{3p} and Na_{3d} states do not play a significant role for the metallicity of Na_3N resulting within DFT-LDA.

The right panel of Fig. 5 shows the orbital-resolved Na_3N band structure resulting from our SIC calculations. From the band markings according to the Mullikan orbital decomposition it becomes apparent that the inclusion of self-interaction corrections significantly reduces the previously discussed mixture of N_{2p} and Na_{3s} states around the Fermi level so that a gap opens.

Potassium nitride (K_3N) is the third compound in the row of alkali-metal nitrides addressed in this work. It exists in a low-density anti- TiI_3 crystal structure (space group $P6_3/mcm$) with lattice constants⁵⁶ of $a=7.80$ Å and $c=7.59$ Å. A top view of the lattice is shown in Fig. 6. This structure can be considered as hexagonal columns consisting of K_3N , in which the K and N atoms are ionically bonded. The length of the K-N bond is 2.78 Å. Within the potassium planes, the K atoms form trigonal arrays with a mutual distance of 3.51 Å. To accurately represent the more extended bulk states in this fairly open structure, we place 20 slowly-decaying s -type Gaussians in the unit cell. They are located in the same four planes as the K and N atoms of the K_3N columns (see side view in Fig. 6) and are stacked on five respective columns of orbitals. These columns pierce the top view of the lattice in Fig. 6 in the middle between neighboring K_3N units (three of them) and in the middle of the two triangles formed by the K_3N units (the other two).

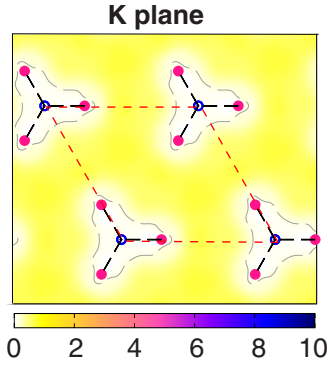


FIG. 7. (Color online) Charge density contours (in $10^{-2}a_B$) of the occupied K -derived state at the Γ point of the hexagonal Brillouin zone at $E = -0.81$ eV (see right panel of Fig. 3, for reference). The density is shown in a $[100]$ - $[010]$ plane containing one potassium layer. Filled rose and open blue circles represent positions of K atoms within and N atoms above and below the plotting plane.

The band structure of K_3N is shown in the right panel of Fig. 3. Obviously, K_3N turns out to be metallic even after inclusion of self-interaction corrections. Also in this case, there is a low-lying N $2s$ band (see Table II). The lowest bands shown in the figure can mainly be attributed to occupied N $2p$ states. They exhibit only a very small dispersion, which is due to the rather large unit cell. Above the Fermi level there is a group of bands that shows similarities to loosely bound, almost free-electron-like s bands extending down in energy to -0.81 eV at Γ . They originate from K atoms. Thus SIC leads to a certain separation of the K $4s$ and N $2p$ bands but it is not as complete as the related separation of the Na $3s$ and N $2p$ bands in Na_3N . The situation resembles more the LDA result for Na_3N in the left panel of Fig. 5 where the Na $3s$ and N $2p$ bands overlap near Γ .

Along the high-symmetry lines on the $k_z = 0$ plane from Γ to K and from M to Γ of the hexagonal Brillouin zone, the lowest of the free-electron-like bands is resonant in energy with the N $2p$ bands leading to the metallicity of K_3N according to our calculations. In our results, the columns at the corners of the hexagonal base plane appear bonded together by metallic electrons between K atoms over a distance of 5.15 Å. This peculiar atomic structure has interesting consequences on the electronic structure. Figure 7 shows charge-density contours of the lowest occupied free-electron-like state at Γ . The density is rather delocalized and fills the empty space between the columns. The free-electron-like bands in the right panel of Fig. 3 can be attributed to this charge density and the associated metallic binding between the stacked K_3N columns on the hexagonal lattice. The mixture of the ionic intracolumn bonding and the metallic intercolumn binding manifests itself in the overlap of the metallic and ionic bands near the Fermi energy. The SIC effects turn out to be less pronounced for K_3N . Nevertheless, they have some influence on the band structure as can be exemplified for selected points in the hexagonal Brillouin zone. The direct gap, e.g., at the A point opens up from 0.35 eV in LDA to 0.72 eV in SIC. To the best of our knowledge, there are no experimental band-structure data available on the highly fragile K_3N for comparison, as yet.

From a chemical point of view, K_3N is expected to be ionic in accord with the formulation $(K^+)_3N^{3-}$ and thus its electronic structure should feature a band gap between the filled N $2p$ and empty K $4s$ states. However, the self-interaction corrections alone, as employed in this work, are not sufficient to open up such a gap, perhaps due to the remaining underestimation as also in the related Na_3N with the expected formulation $(Na^+)_3N^{3-}$. This aspect of the electronic structure remains to be resolved by further experiments or by more advanced calculations.

IV. SUMMARY

We have presented the bulk electronic structure of alkali-metal fluorides, oxides, and nitrides resulting from density-functional theory including self-interaction corrections by employing corresponding pseudopotentials. The calculations are not more demanding than standard DFT-LDA calculations. Except for K_3N , all other alkali-metal fluorides (MF), oxides (M_2O), and nitrides (M_3N) with $M = Li, Na,$ and K turn out to be semiconductors or insulators. In particular, we have analyzed the band structure of Na_3N in more detail since this compound has been synthesized more recently and was shown to be a semiconductor much in contrast to the results of DFT-LDA calculations which find Na_3N to be metallic. On the contrary, our DFT-SIC results clearly corroborate that Na_3N is a semiconductor. In general, our DFT-SIC results for all compounds studied are in good agreement with available experimental data and with the results of calculations going beyond DFT-LDA, such as correlation-corrected Hartree-Fock or GW quasiparticle calculations. The latter have been restricted so far to the fluorides, however. K_3N results as a metal both from our LDA as well as from our SIC calculations. According to our results, this appears to originate from the peculiar lattice structure of K_3N giving rise to a mixed metallic-ionic bonding. More advanced calculations, such as many-body quasiparticle band-structure calculations, might be necessary to eventually clarify this point. They are, however, beyond the scope of this work.

ACKNOWLEDGMENTS

The authors thank O. Gunnarsson for helpful comments. G. V. V. is also grateful to A. Simon for his support.

APPENDIX

In Sec. III we have presented electronic properties of alkali-metal fluorides, oxides, and nitrides, as calculated at the experimental lattice constants (a_{exp}), to allow for a most meaningful direct comparison of LDA and SIC results and a clear identification of the SIC effects on the band structures. In addition, the use of experimental lattice constants appears to be the most realistic for comparison with experiment. If one were to use theoretical lattice constants (a_{th}), which depend on the theoretical method employed, their differences would have an additional effect on the band structures obscuring the pure SIC effect to a certain extent.

To identify this combined effect we have first calculated the lattice constants of the investigated solids within LDA

TABLE III. Calculated lattice constants (in Å) and bulk moduli (in Mbar) resulting from our LDA and SIC calculations in comparison with other theoretical and experimental results.

		LDA	SIC	Other	Exp
LiF	<i>a</i>	3.97	3.91	3.91 ^a ,4.03 ^b	3.99 ^c
	<i>B</i>	0.80	0.95	0.87 ^a ,0.76 ^b	0.77 ^d
NaF	<i>a</i>	4.52	4.44	4.51 ^a ,4.63 ^b	4.57 ^c
	<i>B</i>	0.64	0.72	0.63 ^a ,0.51 ^b	0.54 ^d
KF	<i>a</i>	5.20	5.13	5.49 ^b	5.29 ^c
	<i>B</i>	0.50	0.65	0.30 ^b	0.36 ^d
Li ₂ O	<i>a</i>	4.52	4.50	4.53 ^e ,4.57 ^f	4.62 ^g
	<i>B</i>	0.88	0.91	0.95 ^e ,0.95 ^f	0.89 ^h
Na ₂ O	<i>a</i>	5.35	5.29	5.47 ^e ,5.48 ^f	5.56 ^g
	<i>B</i>	0.62	0.67	0.59 ^e ,0.61 ^f	
K ₂ O	<i>a</i>	6.46	6.42	6.36 ^e	6.45 ^g
	<i>B</i>	0.30	0.34	0.33 ^e	
Li ₃ N	<i>a</i>	3.56	3.55	3.51 ⁱ	3.65 ^j
	<i>c</i>	3.80	3.79	3.75 ⁱ	3.87 ^j
	<i>B</i>	0.60	0.61		
Na ₃ N	<i>a</i>	4.57	4.56		4.73 ^k
	<i>B</i>	0.27	0.28		
K ₃ N	<i>a</i>	7.76	7.89	7.65 ^l	7.80 ^l
	<i>c</i>	7.29	7.10	7.50 ^l	7.59 ^l
	<i>B</i>	0.19	0.18		

^afrom Ref. 57 LDA.

^bfrom Ref. 58 Hartree-Fock.

^cfrom Ref. 36.

^dfrom Ref. 59.

^efrom Ref. 47 LDA.

^ffrom Ref. 60 Hartree-Fock.

^gfrom Ref. 45.

^hfrom Ref. 61.

ⁱfrom Ref. 62 LDA.

^jfrom Ref. 51.

^kfrom Ref. 1.

^lfrom Ref. 56 LDA, Expt.

and SIC. In Table III we summarize optimized lattice constants and bulk moduli for the nine bulk crystals studied. While LDA is known to underestimate lattice constants of common elemental, III-V and II-VI semiconductors only by roughly 1%, in the case of the alkali-metal fluorides, oxides, and nitrides the respective underestimates span a range from 0.5% to about 4% (see Table III). This can be viewed as an indication that the calculation of structural properties of the latter, partially much more ionic materials, is more intricate. This seems to apply to K₃N, in particular.

The lattice constants resulting within SIC are even somewhat smaller than those resulting from LDA. This appears to be related to the fact that both term values of the anions are drastically lowered relative to those of the cations due to SIC by similar amounts (see Table I). As a consequence, the atomic 2*s* and 2*p* orbitals of the anions become more localized in SIC than in LDA and the lattice constants are reduced accordingly. The underestimate of the lattice constants in

TABLE IV. Slope *S* of the variation of calculated band gaps with lattice constants (in eV/Å) according to Eq. (1).

	LDA	SIC
LiF	6.21	7.10
NaF	3.53	4.49
KF	2.22	3.00
Li ₂ O	1.23	1.97
Na ₂ O	1.99	2.88
K ₂ O	0.97	1.70
Li ₃ N	0.97	1.22
Na ₃ N	no gap	0.38
K ₃ N	no gap	no gap

LDA and SIC results in respective overestimates of the bulk moduli, as compared to experiment. We note in passing that our SIC approach yields larger lattice constants than LDA for IIB-VI semiconductor compounds,⁹ group III-nitrides,¹⁰ silicon carbide polytypes,¹² and earth-alkali metal oxides¹⁴ which are in close agreement with experiment. In all of these cases, SIC also leads to a stronger localization of anionic orbitals. This does not give rise to smaller lattice constants, however, since the stronger orbital localization is accompanied by a partial weakening of the bonds in these materials giving rise to an increase in lattice constants. In the alkali-metal fluorides, oxides, and nitrides studied in this work, the valence bands are built up exclusively from anion orbitals while the cation orbitals give rise to the lower conduction bands. As a result, there is no reduction in ionic bonding and no increase in lattice constants involved when the anion orbitals become more localized.

As is well known, energy gaps are sensitive to the lattice constants and to the theoretical method used to calculate them. Very recently, for example, von Lilienfeld and Schultz⁶³ have investigated in great detail the sensitivity of the band gaps of GaAs, GaP, and GaN on pseudopotentials and lattice constants where the Ga 3*d* semicore states are of particular importance. Concerning the materials studied in this work, we find the band gaps to vary linearly with the lattice constants around $E_g(a_{\text{exp}})$. The dependence of E_g on the lattice constant *a* can be described as

$$E_g(a) = E_g(a_{\text{exp}}) + (a_{\text{exp}} - a)S, \quad (1)$$

where *S* is the slope. The resulting slopes are given in Table IV in eV/Å. For the hexagonal Li₃N the slope is calculated at c_{exp} . Note that the differences between measured and calculated lattice constants are only in the order of 0.1 Å in most cases. The gap dependence on lattice constants turns out to be stronger in SIC than in LDA and it is largest for the most ionic solids in the studied material class. With the lattice constants in Table III and the slopes in Table IV the band gaps for the LDA and SIC lattice constants can easily be calculated. For example, the largest effect of the lattice constants occurs for the gap of LiF. It results as 8.5 and 14.7 eV from LDA and SIC at a_{exp} , respectively, (see Table II) while the LDA gap at $a_{\text{th}}^{\text{LDA}}$ is 8.6 eV and the SIC gap at $a_{\text{th}}^{\text{SIC}}$

is 15.3 eV. Thus in the former case the pure SIC-induced opening of the gap amounts to 6.2 eV, while in the latter case the combined influence of the lattice constants and of SIC opens the gap by 6.7 eV seemingly increasing the SIC effect by 0.5 eV. Nevertheless, also the gap energies at the different

theoretical lattice constants clearly reveal the superiority of SIC as compared to LDA. In any case, we consider it to be most realistic to use the experimental lattice constants when the results are to be compared with experiment, as we have done in Sec. III.

*baumeier@uni-muenster.de

- ¹D. Fischer and M. Jansen, *Angew. Chem.* **114**, 1831 (2002); *Angew. Chem., Int. Ed.* **41**, 1755 (2002).
- ²G. V. Vajenine, *Inorg. Chem.* **46**, 5146 (2007).
- ³G. V. Vajenine, *Solid State Sci.* **10**, 450 (2008).
- ⁴J. P. Perdew and A. Zunger, *Phys. Rev. B* **23**, 5048 (1981).
- ⁵A. Svane and O. Gunnarsson, *Phys. Rev. B* **37**, 9919 (1988); *Phys. Rev. Lett.* **65**, 1148 (1990); A. Svane, *ibid.* **68**, 1900 (1992); **72**, 1248 (1994).
- ⁶W. M. Temmerman, Z. Szotek, and H. Winter, *Phys. Rev. B* **47**, 1184 (1993).
- ⁷Z. Szotek, W. M. Temmerman, and H. Winter, *Phys. Rev. B* **47**, 4029 (1993); *Phys. Rev. Lett.* **72**, 1244 (1994).
- ⁸M. Arai and T. Fujiwara, *Phys. Rev. B* **51**, 1477 (1995).
- ⁹D. Vogel, P. Krüger, and J. Pollmann, *Phys. Rev. B* **52**, R14316 (1995); **54**, 5495 (1996).
- ¹⁰D. Vogel, P. Krüger, and J. Pollmann, *Phys. Rev. B* **55**, 12836 (1997).
- ¹¹A. Filippetti and N. A. Spaldin, *Phys. Rev. B* **67**, 125109 (2003).
- ¹²B. Baumeier, P. Krüger, and J. Pollmann, *Phys. Rev. B* **73**, 195205 (2006).
- ¹³C. D. Pemmaraju, T. Archer, D. Sánchez-Portal, and S. Sanvito, *Phys. Rev. B* **75**, 045101 (2007).
- ¹⁴B. Baumeier, P. Krüger, and J. Pollmann, *Phys. Rev. B* **75**, 045323 (2007); **76**, 205404 (2007).
- ¹⁵B. Baumeier, P. Krüger, and J. Pollmann, *Phys. Rev. B* **76**, 085407 (2007).
- ¹⁶L. Kleinman and D. M. Bylander, *Phys. Rev. Lett.* **48**, 1425 (1982).
- ¹⁷D. M. Ceperley and B. J. Alder, *Phys. Rev. Lett.* **45**, 566 (1980).
- ¹⁸D. R. Hamann, *Phys. Rev. B* **40**, 2980 (1989).
- ¹⁹S. G. Louie, S. Froyen, and M. L. Cohen, *Phys. Rev. B* **26**, 1738 (1982).
- ²⁰We use as decay constants (in atomic units) 0.30, 1.34 and 6.00 for Li, 0.16, 0.30, and 0.60 for Na, 0.16, 0.37, and 0.88 for K, 0.20, 0.95, and 4.50 for F, 0.25, 1.00 and 3.70 for O, and 0.31, 1.36, and 6.00 for N. For the additional Gaussian orbitals localized in the empty regions, we use 0.18 as the decay constant.
- ²¹H. J. Monkhorst and J. D. Pack, *Phys. Rev. B* **13**, 5188 (1976).
- ²²The actual number of special k -points in the respective irreducible wedges of the bulk Brillouin zones are 44 (LiF), 28 (NaF), and 19 (KF), 28 (Li₂O), 19 (Na₂O), and 10 (K₂O), as well as 32 (Li₃N), 10 (Na₃N), and 8 (K₃N).
- ²³W. C. Martin, A. Musgrove, S. Kotochigova, and J. E. Sansonetti, *Ground Levels and Ionization Energies for the Neutral Atoms* (National Institute of Standards and Technology, Gaithersburg, MS), available at <http://physics.nist.gov/IonEnergy>; see also W. C. Martin and W. L. Wiese, in *Atomic, Molecular, and Optical Physics Handbook*, edited by G. W. F. Drake (AIP, Woodbury, NY, 1996), Chap. 10, p. 135.
- ²⁴R. O. Jones and O. Gunnarsson, *Rev. Mod. Phys.* **61**, 689 (1989).
- ²⁵The atomic SIC pseudopotentials and the prescription for their transfer to the solids can be obtained from the authors on demand.
- ²⁶D. M. Roessler and W. C. Walker, *J. Phys. Chem. Solids* **28**, 1507 (1967).
- ²⁷E. L. Shirley, L. J. Terminello, J. E. Klepeis, and F. J. Himpsel, *Phys. Rev. B* **53**, 10296 (1996).
- ²⁸M. Piacentini, *Solid State Commun.* **17**, 697 (1975).
- ²⁹S. Nakai and T. Sagawa, *J. Phys. Soc. Jpn.* **26**, 1427 (1969).
- ³⁰J. E. Eby, K. J. Teegarden, and D. B. Dutton, *Phys. Rev.* **116**, 1099 (1959).
- ³¹K. Teegarden and G. Baldini, *Phys. Rev.* **155**, 896 (1967).
- ³²T. Tomiki and T. Miyata, *J. Phys. Soc. Jpn.* **27**, 658 (1969).
- ³³Y. Ishii, J. Murakami, and M. Itoh, *J. Phys. Soc. Jpn.* **68**, 696 (1999).
- ³⁴W. Rauch, *Z. Phys.* **116**, 652 (1940).
- ³⁵H. Brendecke and W. Bludau, *J. Appl. Phys.* **50**, 4743 (1979).
- ³⁶W. G. Wyckoff, *Crystal Structures*, 2nd ed. (Wiley, New York, 1968), Vol. 1.
- ³⁷F. Perrot, *Phys. Status Solidi B* **52**, 163 (1972).
- ³⁸A. B. Kunz, *Phys. Rev. B* **26**, 2056 (1982).
- ³⁹M. Berrondo and J. F. Rivas-Silva, *Int. J. Quantum Chem.* **57**, 1115 (1996).
- ⁴⁰J. A. Soininen and E. L. Shirley, *Phys. Rev. B* **61**, 16423 (2000).
- ⁴¹N.-P. Wang, M. Rohlfing, P. Krüger, and J. Pollmann, *Phys. Rev. B* **67**, 115111 (2003).
- ⁴²S. C. Erwin and C. C. Lin, *J. Phys. C* **21**, 4285 (1988).
- ⁴³R. T. Poole, J. G. Jenkin, J. Liesegang, and R. C. G. Leckey, *Phys. Rev. B* **11**, 5179 (1975).
- ⁴⁴G. K. Wertheim, J. E. Rowe, D. N. E. Buchanan, and P. H. Citrin, *Phys. Rev. B* **51**, 13675 (1995).
- ⁴⁵E. Zintl, A. Harder, and B. Dauth, *Z. Elektrochem. Angew. Phys. Chem.* **40**, 588 (1934).
- ⁴⁶M. M. Islam, T. Bredow, and C. Minot, *J. Phys. Chem. B* **110**, 9413 (2006).
- ⁴⁷R. D. Eithiraj, G. Jaiganesh, and G. Kalpana, *Physica B (Amsterdam)* **396**, 124 (2007).
- ⁴⁸E. A. Mikajlo, K. L. Nixon, V. A. Coleman, and M. J. Ford, *J. Phys.: Condens. Matter* **14**, 3587 (2002).
- ⁴⁹E. A. Mikajlo, K. L. Nixon, and M. J. Ford, *J. Phys.: Condens. Matter* **15**, 2155 (2003).
- ⁵⁰E. A. Mikajlo and M. J. Ford, *J. Phys.: Condens. Matter* **15**, 6955 (2003).
- ⁵¹A. Rabenau and H. Schulz, *J. Less-Common Met.* **50**, 155 (1976).
- ⁵²H. J. Beister, S. Haag, R. Kniep, K. Strößner, and K. Syassen, *Angew. Chem., Int. Ed. Engl.* **27**, 1101 (1988).
- ⁵³G. Kerker, *Phys. Rev. B* **23**, 6312 (1981).

- ⁵⁴P. Blaha, J. Redinger, and K. Schwarz, *Z. Phys. B: Condens. Matter* **57**, 273 (1984).
- ⁵⁵M. Seel and R. Pandey, *Int. J. Quantum Chem.* **40**, 461 (1991).
- ⁵⁶D. Fischer, Z. Cancarevic, J. C. Schön, and M. Jansen, *Z. Anorg. Allg. Chem.* **630**, 156 (2004).
- ⁵⁷V. N. Staroverov, G. E. Scuseria, J. Tao, and J. P. Perdew, *Phys. Rev. B* **69**, 075102 (2004).
- ⁵⁸M. Prencipe, A. Zupan, R. Dovesi, E. Apra, and V. R. Saunders, *Phys. Rev. B* **51**, 3391 (1995).
- ⁵⁹S. Haussühl, *Z. Phys.* **159**, 223 (1960).
- ⁶⁰A. Shukla, M. Dolg, P. Fulde, and H. Stoll, *J. Chem. Phys.* **108**, 8521 (1998).
- ⁶¹S. Hull, T. W. D. Farley, W. Hayes, and M. T. Hutchings, *J. Nucl. Mater.* **160**, 125 (1988).
- ⁶²A. C. Ho, M. K. Granger, A. L. Ruoff, P. E. Van Camp, and V. E. Van Doren, *Phys. Rev. B* **59**, 6083 (1999).
- ⁶³O. A. von Lilienfeld and P. A. Schultz, *Phys. Rev. B* **77**, 115202 (2008).